Dual-color fluorescence imaging distinguishes tumor cells from induced host angiogenic vessels and stromal cells

Meng Yang*, Lingna Li*, Ping Jiang*, A. R. Moossa†, Sheldon Penman‡, and Robert M. Hoffman*†§

*AntiCancer, 7917 Ostrow Street, San Diego, CA 92111; †Department of Surgery, University of California at San Diego, La Jolla, CA 92103-8220; and ‡Department of Biology, Massachusetts Institute of Technology, Cambridge, MA 02139-4307

Contributed by Sheldon Penman, September 24, 2003

We have developed a simple yet powerful technique for delineating the morphological events of tumor-induced angiogenesis and other tumor-induced host processes with dual-color fluorescence. The method clearly images implanted tumors and adjacent stroma, distinguishing unambiguously the host and tumor-specific components of the malignancy. The dual-color fluorescence imaging is effected by using red fluorescent protein (RFP)-expressing tumors growing in GFP-expressing transgenic mice. This model shows with great clarity the details of the tumor–stroma interaction, especially tumor-induced angiogenesis and tumor-infiltrating lymphocytes. The GFP-expressing tumor vasculature, both nascent and mature, could be readily distinguished interacting with the RFP-expressing tumor cells. GFP-expressing dendritic cells were observed contacting RFP-expressing tumor cells with their dendrites. GFP-expressing macrophages were observed engulfing RFP-expressing cancer cells. GFP lymphocytes were seen surrounding cells of the RFP tumor, which eventually regressed. Dual-color fluorescence imaging visualizes the tumor–host interaction by whole-body imaging and at the cellular level in fresh tissues, dramatically expanding previous studies in fixed and stained preparations.

GFP mouse–RFP tumor | host vessels | tumor-infiltrating lymphocytes | macrophages | dendritic cells

The current interest in angiogenesis is the most recent development in the ongoing study of tumor–host interactions. Although much recent research has focused on the genetic makeup of the tumors themselves, it has long been apparent that host tissues also participate in the phenomena of malignancy. Studies pioneered by Judah Folkman showed that the development of tumor-induced vasculature was essential for tumor growth beyond an initial small size (1). This remarkable finding afforded important new insights into the mechanisms regulating tumor growth and, perhaps most importantly, indicated that newly induced blood vessels offered promising new therapeutic targets. The findings that tumor-induced angiogenesis is a critical determinant of tumor growth and that newly formed vessels offer an especially promising target for chemotherapy have greatly increased the importance understanding the tumor–host interaction.

One of the earliest indications of the importance of host tissue to tumor growth was the selectivity of metastatic seeding. Target tissues most often were characteristic of the originating tumor. Such metastasis was described in the "seed and soil" hypothesis by Paget (2) more than 100 years ago. Paget (2) proposed that tumor cells, or "seeds," were randomly disseminated by vascular routes, but that metastatic deposits grew only on permissive organs, i.e., the "soil." Paget hypothesized that tumors act together with the distant organ to effect tumor metastases. Fidler (3–6) developed the concept of the tumor microenvironment in the host tissue necessary for growth promotion. The metastatic host microenvironment consists of critical host endothelial cells that form new blood vessels, epithelial cells, lymphocytes, platelets, macrophages, fibroblasts, and other cell types interacting with tumor cells and enabling a metastasis to grow. Fidler (3–6) noted that the microenvironments of different organs (the soil) are biologically unique and that growth of potentially metastatic cells depends on interaction of these cells with host cells. The host may resist tumor growth by both immune and other mechanisms (7).

Thus, solid tumors proliferate in a complex association with the stromal tissue, which provides the vascular supply to the tumor as the result of angiogenesis. Unfortunately, the factors regulating stromal element induction, as well as the influences these elements have on tumor growth, are poorly understood. The paucity of information about the interaction between tumor and host is due largely to the absence of suitable models that allow visualization and precise study of the tumor–host interaction in the living state.

A number of attempts have been made to visualize the tumor–host interaction. To study tumor angiogenesis, Fukumura *et al.* (8) and Brown *et al.* (9) have used transgenic mice that express the GFP under the control of the human vascular endothelial cell growth factor promoter. After implantation of solid tumors, highly fluorescent fibroblasts were observed surrounding and infiltrating the tumor mass. When spontaneous mammary tumors developed in these mice, GFP was visualized in fibroblasts surrounding the neoplastic nodules but not in the tumor cells themselves. Thus, the vascular endothelial cell growth factor promoter of nontransformed cells is strongly activated by the tumor microenvironment (8, 9).

Unfortunately, the previous models did not enable simultaneous imaging of tumor and host cells. However, when Okabe *et al.* (10) produced transgenic mice with GFP under the control of a chicken β-actin promoter and cytomegalovirus enhancer, it became possible to visualize all of the host cells that can interact with the tumor. All of the tissues from these transgenic mice, with the exception of erythrocytes and hair, fluoresce green.

Tumor cells to be transplanted in the GFP mouse were made visible by transforming them with the red fluorescent protein (RFP) (11). To gain further insight into the tumor–host interaction in the living state, including tumor angiogenesis and immunology, we have visualized RFP-expressing tumors transplanted in the GFP-expressing transgenic mice under dual-color fluorescence imaging and microscopy. Dual-color fluorescence makes it possible to visualize the tumor growth in the host by whole-body imaging as well as to visibly distinguish interacting tumor and host cells in fresh tissue. The results reported here afford a powerful means of both visualizing and distinguishing the components of the host–tumor interaction.

Materials and Methods

GFP Transgenic Animals. Transgenic C57/B6-GFP mice (10) were obtained from the Research Institute for Microbial Diseases

Abbreviation: RFP, red fluorescent protein.

§To whom correspondence should be addressed. E-mail: all@anticancer.com.

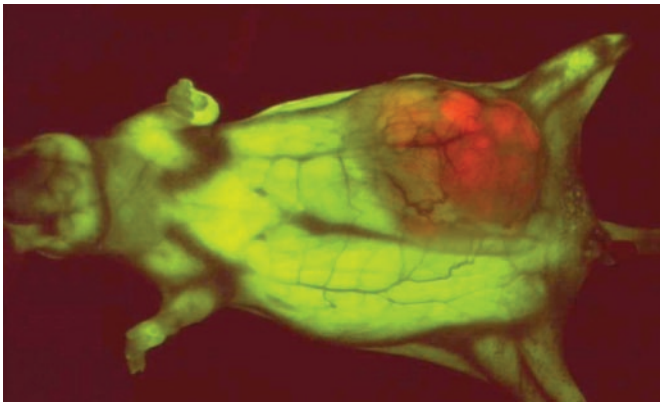

Fig. 1. Whole-body image of orthotopically growing HCT 116-RFP human colon cancer in GFP nude mouse. Image was acquired in a fluorescence light box with a CCD camera 10 weeks after orthotopic implantation of HCT 116-RFP cells. See *Materials and Methods* for details.

(Osaka University, Osaka). The C57/B6-GFP mice expressed the *Aequorea victoria* GFP under the control of the chicken β-actin promoter and cytomegalovirus enhancer. All of the tissues from this transgenic line, with the exception of erythrocytes and hair, fluoresced green under excitation light. The GFP gene, regulated as described above, was crossed into nude mice on the C57/B6 background. Both immunocompetent and nude GFP transgenic mice were used in the present study.

Expression Vectors. The pLNCX$_2$ vector was purchased from Clontech. The pLNCX$_2$ vector contains the neomycin resistance gene for antibiotic selection in eukaryotic cells. The RFP (DsRed2, Clontech) was inserted in the pLNCX$_2$ vector at the *Egl*II and *Not*I sites.

RFP Vector Production. For retroviral transduction, PT67, an NIH 3T3-derived packaging cell line expressing the 10 Al viral envelope, was purchased from Clontech. PT67 cells were cultured in DMEM (Irvine Scientific) supplemented with 10% heat-inactivated FBS (Gemini Biological Products, Calabasas, CA). For vector production, packaging cells (PT67), at 70% confluence, were incubated with a precipitated mixture of DOTAP reagent (Boehringer Mannheim) and saturating amounts of pLNCX$_2$-DsRed2 plasmid for 18 h. Fresh medium was replenished at this time. The cells were examined by fluorescence microscopy 48 h posttransfection. For selection of brightly fluorescing cells producing high-titer retroviral supernatants, the RFP-expressing packaging cells were cultured in the presence of 500–2,000 μg/ml G418 increased in a stepwise manner (Life Technologies, Grand Island, NY) for 7 days.

RFP Gene Transduction of Tumor Cell Lines. For RFP gene transduction, 20% confluent rodent B16F0 melanoma cells, MMT060562 mammary tumor cells, Dunning prostrate carcinoma cells, as well as human PC-3 prostate carcinoma cells and HCT-116 colon cancer cells were incubated with a 1:1 precipitated mixture of retroviral supernatants of PT67 cells and RPMI 1640 or other culture media (GIBCO) containing 10% FBS (Gemini Biological Products) for 72 h. Fresh medium was replenished at this time. Tumor cells were harvested with trypsin/EDTA and subcultured at a ratio of 1:15 into selective medium, which contained 50 μg/ml G418. To select brightly fluorescent cells, the level of G418 was increased to 800 μg/ml in a stepwise manner. Clones expressing RFP were isolated with cloning cylinders (Bel-Art Products) by trypsin/EDTA and were

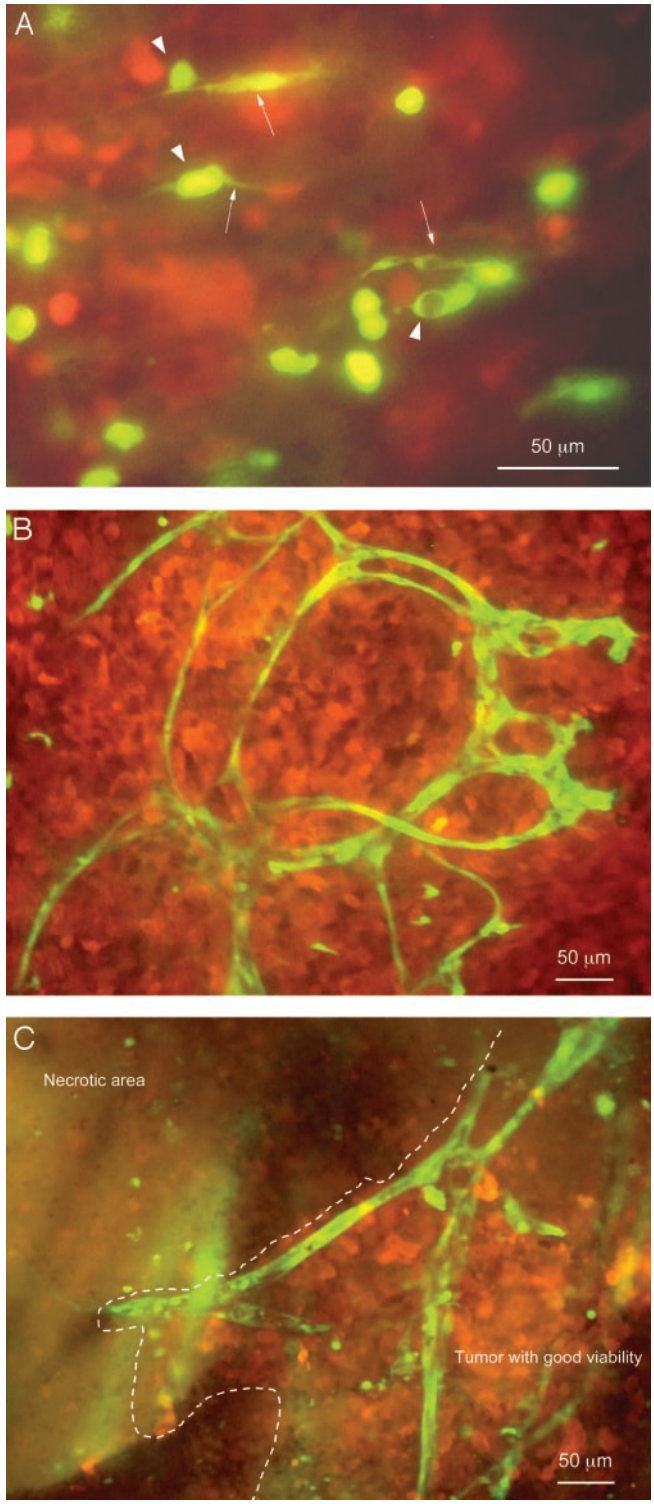

Fig. 2. Visualization of angiogenesis in live tumor tissue 3 weeks after s.c. injection of B16F10-RFP melanoma cells in the transgenic GFP mouse. (*A*) Visualization of angiogenesis onset and development imaged in live tumor tissue. Host-derived GFP-expressing fibroblast cells (arrows) and endothelial cells (arrowheads) are shown forming new blood vessels in the RFP-expressing B16F10 melanoma. (*B*) Well developed, host-derived GFP-expressing blood vessels are visualized in the RFP-expressing mouse melanoma. (*C*) Tumor vasculature in viable tumor tissue and necrotic tumor tissue in the same tumor mass are visualized. GFP-expressing tumor vasculature can be readily identified in the area where the tumor tissue maintained good viability; however, only remnants of GFP-expressing vasculature can be visualized in the necrotic area. (Scale bars, 50 μm.) See *Materials and Methods* for details.

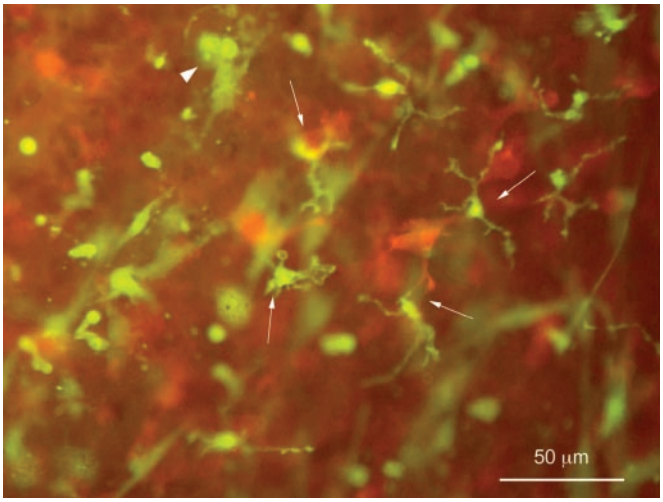

Fig. 3. Visualization of the interaction of host dendritic cells and tumor cells in fresh tumor tissue. Many host-derived GFP-expressing dendritic cells directly contacting B16F10-RFP melanoma cells with their dendrites (arrows) are visualized. Dendritic cell–lymphocyte clusters can be seen in certain regions of the image (arrowheads) 3 weeks after tumor implantation. (Scale bar, 50 μm.)

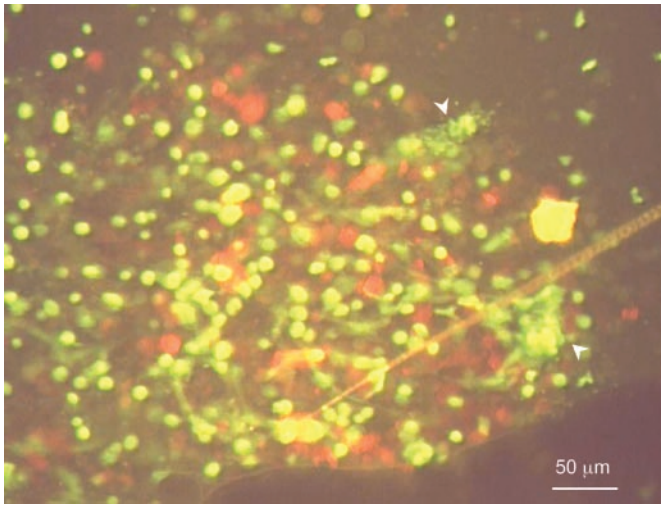

Fig. 4. Visualization of extensive host lymphocyte infiltration in fresh tumor tissue. Numerous host-derived GFP-expressing immune cells, mainly lymphocytes, are infiltrating into the tumor mass and forming immune clusters (arrowheads) in orthotopically implanted MTT060562-RFP mouse breast cancer by day 3 after tumor implantation. (Scale bar, 50 μm.)

amplified and transferred by conventional culture methods in the absence of selective agent.

RFP-Expressing Cutaneous Melanoma Model. Six-week-old male C57/B6-GFP mice were injected s.c. with 10^6 RFP-expressing mouse B16F0 melanoma cells. Cells were first harvested by trypsinization and washed three times with cold serum-containing medium and then kept on ice. Cells were inoculated by intradermal injection of the dorsal skin of the animal in a total volume of 50 μl within 40 min of harvesting.

RFP-Expressing Orthotopic Breast Cancer Model. Six-week-old female C57/B6-GFP mice were injected orthotopically with 10^6 RFP-expressing mouse MMT060562 mammary tumor cells. Cells were first harvested by trypsinization and washed three times with cold serum-containing medium and then kept on ice. Cells were injected in the mammary fat pads of the animal in a total volume of 50 μl within 40 min of harvesting.

RFP-Expressing Orthotopic Prostate Cancer Models. Six-week-old male C57/B6-GFP immunocompetent mice were injected orthotopically with a single dose of 5×10^5 RFP-expressing rat Dunning prostate cancer cells. Similarly, C57/B6 GFP nude mice were injected with 10^6 PC-3-RFP human prostate cancer cells. Cells were first harvested by trypsinization and washed three times with cold serum-containing medium and then kept on ice. The cells were injected in a total volume of 30 μm within 40 min of harvesting. The bladder and prostate were exposed after a lower midline abdominal incision. The incision in the abdominal wall was closed with a 6–0 surgical suture in one layer. The animals were kept under isoflurane anesthesia during surgery. All procedures of the operation described above were performed with a $\times 7$ magnification stereomicroscope.

RFP-Expressing Orthotopic Colon Cancer Model. Six-week-old transgenic female GFP nude mice were used as the host for HCT-116-RFP human colon cancer cells. HCT-116-RFP cells were first harvested by trypsinization and washed three times with cold serum-free medium and then resuspended with serum-free RPMI medium 1640. The cells were injected within 40 min of harvesting. After proper exposure of the colon through a lower left abdominal incision, 10^6 HCT-116-RFP cells in 50 μl were injected under the serosa of the descending colon by using a 25-μl syringe (Hamilton). The incision in the abdominal wall was closed with a 6–0 surgical suture in one layer. The animals were kept under ketamine anesthesia during surgery.

Tumor Tissue Sampling. Tumor tissue biopsies were processed from 3 days to 4 weeks after inoculation of tumor cells. Fresh tissue was cut into $\approx$1-mm^3 pieces and pressed on slides for fluorescence microscopy. For analyzing tumor angiogenesis, the tissues were digested with trypsin/EDTA at 37°C for 5 min before examination. After trypsinization, tissues were put on precleaned microscope slides (Fisher Scientific) and covered with another microscope slide.

Whole-Body Imaging. Whole-body imaging (11) was performed in a fluorescent light box illuminated by fiber-optic lighting at 470 nm (Lightools Research, Encinitas, CA). Emitted fluorescence was collected through a long-pass filter GG475 (Chroma Technology, Brattleboro, VT) on a Hamamatsu C5810 three-chip cooled color CCD camera (Hamamatsu Photonics, Bridgewater, NJ). High-resolution images of 1,024/724 pixels were captured directly on an IBM PC. Images were processed for contrast and brightness and analyzed with the use of IMAGE PRO PLUS 3.1 software (Media Cybernetics, Silver Spring, MD).

Fluorescence Imaging Microscopy. An Olympus BH 2-RFCA fluorescence microscope equipped with a mercury 100-W lamp power supply was used. To visualize both GFP and RFP fluorescence at the same time, excitation light was produced through a D425/60 band pass filter, 470 DCXR dichroic mirror. Emitted fluorescence light was collected through a long pass filter GG475 (Chroma Technology). High-resolution images of 1,024/724 pixels were captured by a Hamamatsu C5810 three-chip cooled color CCR camera (Hamamatsu Photonics) (10) and directly stored on an IBM PC. Images were processed for contrast and brightness and analyzed with the use of IMAGE PRO PLUS 4.0 software (Media Cybernetics).

All animal studies were conducted in accordance with the principles and procedures outlined in the National Institutes of Health National Research Council's *Guide for the Care and Use of Laboratory Animals* (available at http://oacu.od.nih.gov/regs/guide/guidex.htm) under assurance number A3873-1.

Animals were kept in a barrier facility under HEPA filtration. Mice were fed with autoclaved laboratory rodent diet (Tecklad LM-485, Western Research Products, Orange, CA).

Results

Whole-Body Imaging of RFP-Expressing Colon Tumor in GFP Mouse. Whole-body imaging in a fluorescence light box visualizes the orthotopically growing RFP-expressing HCT-116 human colon cancer contrasted to the GFP-expressing nude mouse host (Fig. 1). The dual-color imaging system readily distinguishes the tumor from the host, suggesting that fluorescence microscopy of fresh tissue would visually differentiate tumor and host at the cellular level.

Visualizing Angiogenesis Onset and Development in Fresh Tumor Tissue. Dual-color images of early events in tumor angiogenesis induced by an RFP-expressing B16F10 mouse melanoma in the transgenic GFP-expressing mouse are shown in Fig. 2*A*. Host-derived GFP-expressing fibroblast cells (arrows) and endothelial cells (arrowheads) that form nascent blood vessels are seen clearly against the red fluorescent background of the RFP-expressing mouse melanoma. Fig. 2*B* shows well developed, host-derived GFP-expressing blood vessels within the RFP-expressing mouse melanoma.

Fig. 2*C* compares tumor vasculature in viable tumor tissue to necrotic tumor tissue in the same tumor mass. GFP-expressing tumor vasculature can be readily identified in the area where the tumor tissue maintained good viability. In the necrotic area, however, only remnants of GFP-expressing vasculature can be visualized.

The images were acquired 3 weeks after s.c. injection of B16F10-RFP melanoma cells in the GFP mouse.

Visualization of Interaction of Host Dendritic Cells and Tumor Cells in Live Tumor Tissue. Fig. 3 shows many host-derived GFP-expressing dendritic cells directly contacting B16F10-RFP melanoma cells with their dendrites.

Host Lymphocyte Infiltration Visualized in Fresh Tumor Tissue. In the case of orthotopically implanted MTT060562-RFP mouse breast cancer cells, strong immune responses could be observed by day 3 after tumor implantation. Numerous host-derived GFP-expressing lymphocytes are seen infiltrating the RFP-expressing tumor mass (Fig. 4). This apparent immune response is consistent with this tumor's eventual regression.

Visualization of Host Macrophage–Tumor Cell Interaction in Live Tumor Tissue. Fig. 5 shows host macrophages expressing GFP 35 days after orthotopic implantation of human prostate carcinoma cells in the transgenic GFP nude mouse. The host macrophages, identified by morphology, expressing GFP are observed contacting and engulfing prostate cancer cells expressing RFP (Fig. 5).

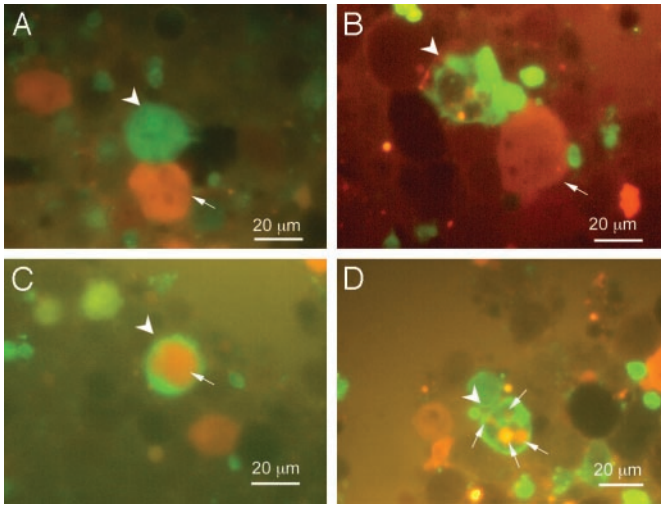

Fig. 5. Visualization of host macrophage–tumor cell interaction in fresh tumor tissue. Images show host macrophages expressing GFP interacting with human PC-3-RFP prostate cancer cells on day 35 after orthotopic implantation of PC-3-RFP cells in the transgenic GFP nude mouse. (*A*) Host GFP macrophage (arrowhead) contacting RFP cancer cell (arrow). (*B*) GFP macrophage (arrowhead) engulfing RFP cancer cell (arrow). (*C*) RFP cancer cell (arrow) engulfed by GFP macrophage (arrowhead). (*D*) RFP cancer cell (arrows) digested by GFP macrophage (arrowhead). (Scale bars, 20 μm.)

Discussion

This dual-color tumor–host interaction model system allows visualization of tumor–host interaction by whole-body imaging as well as in fresh tissue. Both the tumor and the host are uniquely identified by their fluorescence color: RFP for the tumor and GFP for the host. The model has shown the specificity of various types of host cells for the tumor. For example, we have visualized tumor cells being contacted by host dendritic cells, macrophages engulfing tumor cells, and lymphocytes attacking the tumor, which eventually regressed. The dual-color, tumor–host interaction model system allows observation of tumor–host interaction at the single-cell level in fresh tissue, affording further insights into the role of host cells in tumor growth and progression. This may be particularly important for understanding the angiogenic process. The model can be used to elucidate factors whose expression within the tumor or host cells may play a role in malignancy. The model can also be used to develop specific therapeutics that attack or support host cells that affect tumor growth and progression.

We thank Professor Masaru Okabe of Osaka University for the C57/B6-GFP mice. This work was funded in part by National Cancer Institute Grant 1 R43 CA101600-01.

1. Folkman, J. (2003) *Semin. Cancer Biol.* **13,** 159–167.
2. Paget, S. (1889) *Lancet* **1,** 571–573.
3. Fidler, I. J. (2003) *Nat. Rev. Cancer* **3,** 453–458.
4. Fidler, I. J. (2002) *Differentiation* **70,** 498–505.
5. Fidler, I. J. (2001) *J. Natl. Cancer Inst.* **93,** 1040–1041.
6. Fidler, I. J. (2001) *Surg. Oncol. Clin. N. Am.* **10,** 257–269.
7. Krutovskikh, V. (2002) *Semin. Cancer Biol.* **12,** 267–276.
8. Fukumura, D., Xavier, R., Sugiura, T., Chen, Y., Park, E. C., Lu, N., Selig, M., Nielsen, G., Taksir, T., Jain, R. K. & Seed, B. (1998) *Cell* **94,** 715–725.
9. Brown, E. B., Campbell, R. B., Tsuzuki, Y., Xu, L., Carmeliet, P., Fukumura, D. & Jain, R. K. (2001) *Nat. Med.* **7,** 864–868.
10. Okabe, M., Ikawa, M., Kominami, K., Nakanishi, T. & Nishimune, T. (1997) *FEBS Lett.* **407,** 313–319.
11. Hoffman, R. M. (2002) *Lancet Oncol.* **3,** 546–556.